Experimental Investigation into the Compressive Behavior of Steel Columns with Flange Joints in Prefabricated Steel Frame Structures

Jianjun Yang, Huaguo Chen, and Jian Min

***Abstract*—This paper focuses on steel columns with flange joints in prefabricated steel frame structures. To investigate the compressive performance of such steel columns, fifteen specimens were tested. The experimental results indicate that, compared to non-joint columns, the bearing capacity and bending stiffness of high-strength bolt joint columns and bolt tapping columns are less, but they can transfer the compressive load better. The failure mode of the steel columns was ductile failure. This study aims to promote the adoption of prefabricated steel frame structures and the improvement of standards.**

***Index Terms*—Compressive behavior, prefabricated steel frame structure, high-strength bolt joint, bolt tapping joint.**

I. Introduction

Currently, prefabricated steel frame structures, which have proven high quality, can reduce costs and improve housing environmental performance, have received much attention [1]-[6]. Many analytical, numerical and experimental studies concerning such structures are underway.

X.C. Liu et al. proposed a type of bolted-welded beam-column joint for modularized prefabricated multi-rise and high-rise steel structures which maintained relatively good seismic performance [7]. L árus H. L árusson et al. conducted a study on prefabricated composite and modular floor deck panels composed of relatively thin-fiber reinforced concrete slabs connected to steel substructures. The system indicates that the composite construction concept offers flexibility in the assembly process, the ability to adapt to various load and boundary requirements, and efficient utilization of material properties [8]. Wei Jian Zhao et al. studied the properties of a column-to-wall connection in the prefabricated frame-shear wall structure. The results showed that the mechanical properties of the four prefabricated structures are similar to the cast-in-situ structure [9].

Nevertheless, due to the lack of standards in modular high-rise steel structures, prefabricated structures are not extensively used in China. Furthermore, there are few studies on the compressive behavior of steel columns with flange joints in prefabricated steel frame structures, as shown in Fig. 1. Also, it is the joint that is the weak link of the structure, and the connection of the tapping nodes lacks experimental study. Therefore, it is necessary to investigate the steel joint to promote its application.

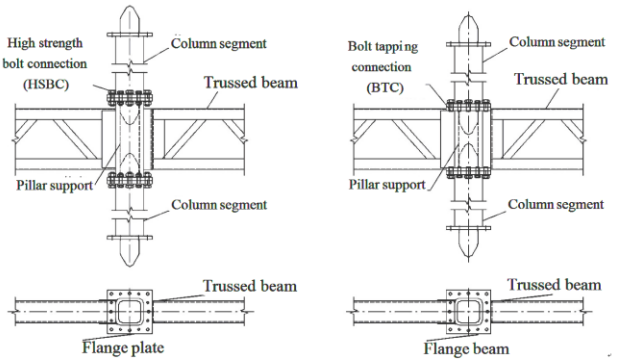

Fig. 1. Beam-column joint.

II. Experimental Program

A. Experiment Design

To examine the compressive performance of steel column joints, this study performed a series of eccentric and axial loading tests for fifteen specimens (nine specimens for eccentric loading tests and six specimens for axial loading tests), as shown in Fig. 2 Table I summarizes all the design parameters of the steel column in the test specimens. The nine columns were divided into three groups (-1D, -2D, -3D), with different thicknesses of 10, 20, and 30mm, respectively, so were the six columns. The thicknesses of the pillar support, the thickness of the column segment, the offset value and the node type were used as variables to investigate the effect on the steel columns. The node types were high-strength bolt connection (HSBC), bolt tapping connection (BTC), and node free connection (NFC).

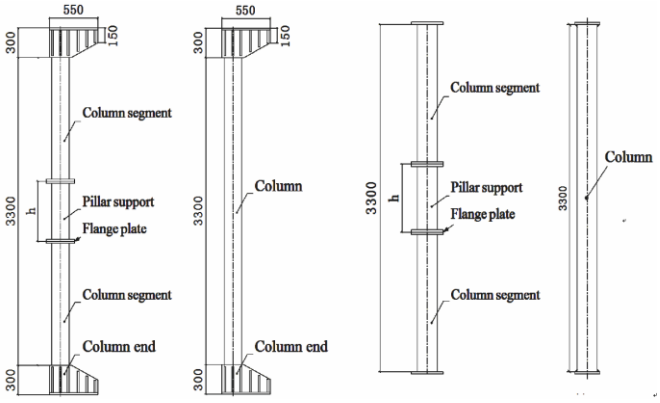

(a) Eccentric compression (b) Axial compression

Fig. 2. Specimen (Unit: mm).

Manuscript received July 1, 2017; revised March 24, 2018. This work was supported in part by Broad Homes Industrial Co. Ltd.

Huaguo Chen and Jianjun Yang are with School of Civil Engineering, Central South University, Changsha 410000, China (e-mail:chuaguo@csu.edu.cn, 578514021@qq.com).

Jian Min is with China Construction Third Bureau First Engineering Co., Ltd., Wuhan 430000, China (e-mail: 387966942@qq.com).

DOI: 10.7763/IJET.2018.V10.1083

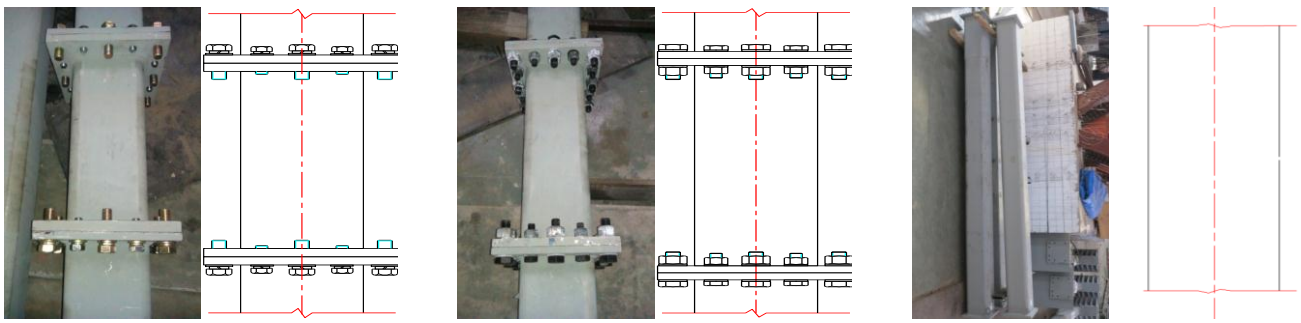

(a) BTC (b) HSBC (c) NFC

Fig. 3. Node type.

TABLE I: SPECIFICATION FOR STEEL COLUMN SPECIMENS

Specimen	The thickness of pillar support (mm)	The thickness of column segment (mm)	Offset value (mm)	Node type (mm)
PY-1D	10	20	300	HSBC
PW-1D	10	20	300	NFC
PYGS-1D	10	20	300	BTC
PY-2D	20	20	300	HSBC
PW-2D	20	20	300	NFC
PYGS-2D	20	20	300	BTC
PY-3D	30	30	300	HSBC
PW-3D	30	30	300	NFC
PYGS-3D	30	30	300	BTC
ZY-1D	10	20	0	HSBC
ZW-1D	10	20	0	NFC
ZY-2D	20	20	0	HSBC
ZW-2D	20	20	0	NFC
ZY-3D	30	30	0	HSBC
ZW-3D	30	30	0	NFC

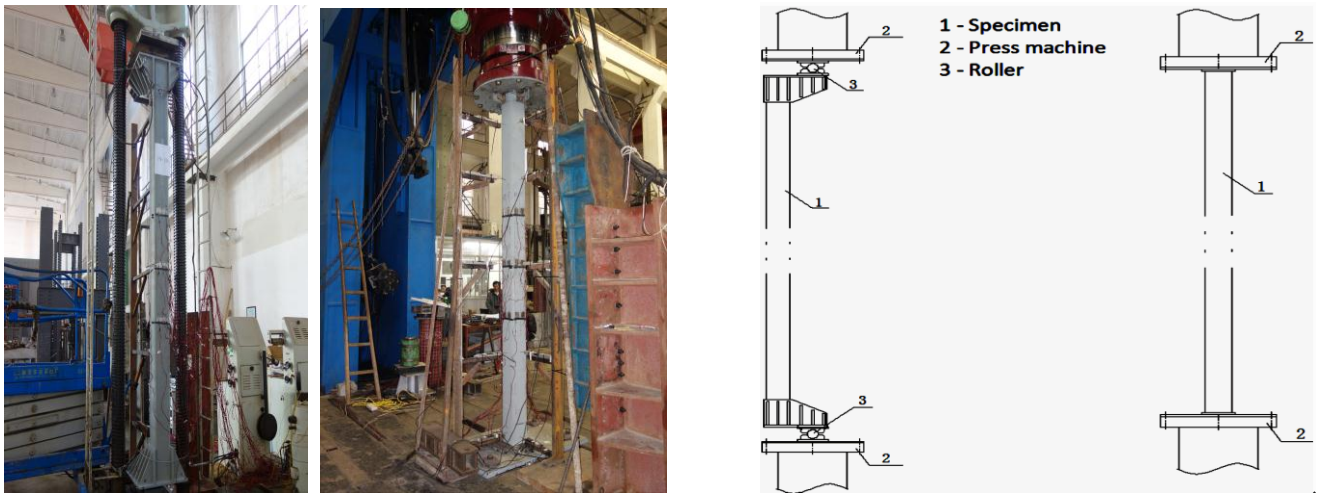

(a) Actual test set-up (b) Design test set-up

Fig. 4. Installation of specimens.

B. Experimental Setup and Instrumentation

Fig. 4 shows the test set-up and a specimen ready for the loading application. The eccentric compression test was conducted indoors under monotonic static loading using a universal testing machine with a capacity of 5000kN. The roller, which could rotate around the free ends of the column without horizontal displacement (perpendicular to steel column), was installed at the upper and lower ends of the specimens. The axial compression test was conducted with a test system with a capacity of 20000kN. Four steel plates were welded to the loading plate of the press machine to limit the horizontal displacement at both ends of the specimen. Therefore, the test set-up could simulate the constraints under eccentric and axial compression.

Fig. 5 shows the strain gauge and displacement meter location. The strain gauges were arranged at the column's mid-span, and 500mm above and below the column's mid-span. In addition, the strain was recorded using the DH3815N static data acquisition system. Two strain gauges were arranged respectively on the compression and tensile side of the specimen under eccentric compression. Also, five strain gauges were arranged on the side of the column. These are numbered ①-⑨. Two strain gauges were arranged on all sides of the specimen under axial compression. These are numbered ①-⑧. To detect the deformation of the specimen, the displacement meter was placed at the middle of the column and at 750mm and 1500mm above and below the middle of the column.

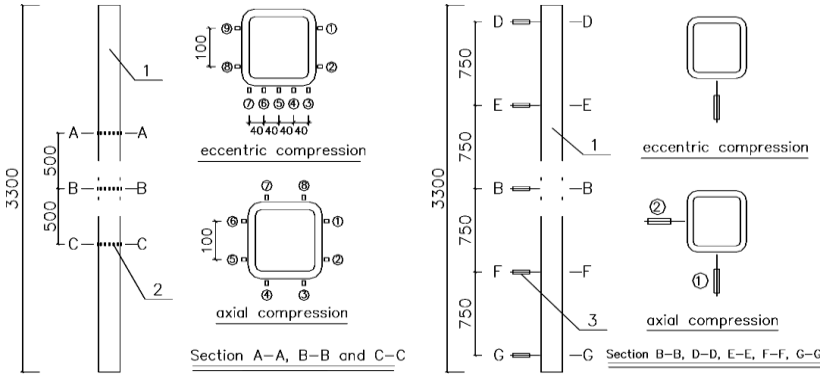

Fig. 5. Layout of strain gauge and displacement meter.

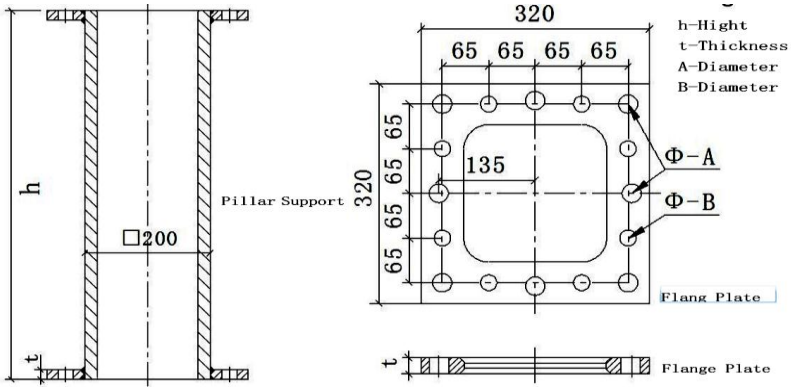

Fig. 6. Schematic diagram of flange (Unit: mm).

TABLE II: FLANGE PARAMETERS

The thicknesses of pillar support	Pillar support (mm)			Pillar support (mm)			Column segment (mm)			Column segment (mm)		
	t	A	B	t	A	B	t	A	B	t	A	B
10mm (-1D)	16	28	24	16	30	26	20	28	24	20	24	20
20mm (-2D)	20	28	28	20	30	26	20	28	24	20	24	20
30mm (-3D)	24	31	28	24	36	30	24	31	28	24	30	24

TABLE III: SPECIFICATIONS, GRADES AND LAYOUT OF BOLTS

Specimen	Bore diameter (mm)		Edge distance of holes (mm)		hole spacing (mm)	Bolt diameter (mm)	Bolt grade (mm)
	FL[a] of pillar support	FL of column segment	FL of pillar support	FL of column segment			
PY-1D	Φ28	Φ24	30	25	65	24/20	M10.9
PW-1D	-	-[b]	-	-	-	-	-
PYGS-1D	Φ30	Φ26	30	25	65	24/20	M8.8
PY-2D	Φ28	Φ24	30	25	65	24/20	M10.9
PW-2D	-	-	-	-	-	-	-
PYGS-2D	Φ30	Φ26	30	25	65	24/20	M8.8
PY-3D	Φ31	Φ28	30	25	65	27/24	M10.9
PW-3D	-	-	-	-	-	-	-
PYGS-3D	Φ36	Φ30	30	25	65	30/24	M8.8
ZY-1D	Φ28	Φ24	30	25	65	24/20	M10.9
ZW-1D	-	-	-	-	-	-	-
ZY-2D	Φ28	Φ24	30	25	65	24/20	M10.9
ZW-2D	-	-	-	-	-	-	-
ZY-3D	Φ31	Φ28	30	25	65	27/24	M10.9
ZW-3D	-	-	-	-	-	-	-

-[a] FL: Flange plate

-[b] Not available

(a) Eccentric compression

(b) Axial compression

Fig. 7. Specimen failure.

C. Experimental Parameters

Q345B Steel was used in this study. The actual mechanical properties of the steel were determined by the Chinese Standard (GB/T 228-2002)[10]. The obtained average elongation, yield and ultimate strength of the columns were 0.31, 375*Mpa* and 529 *Mpa*, respectively.

Table III and Table IV show the schematic diagram and the parameters of the flange plate.

III. Experimental Resu Lts And Analysis

A. Failure Model

Fig. 7 shows the typical steel column at failure under eccentric and axial compression. During the test, the macroscopic failure phenomena of the 12 specimens were similar, with the main results as follows: At the initial stage of loading, the lateral displacement of the specimen increased linearly with the increase of load. The specimen was in the elastic stage. As the load increased to yield load P_y, the specimen began to yield. Note that the load continued to increase, the stiffness of the specimen began to decrease, and the lateral deformation increased rapidly and entered the elastic-plastic stage. Continuing to load until the load began to drop, the failure modes of the three specimens were column yielding but no flange plate bolt slippage was observed. The experimental results of the 15 column specimens, in terms of the yield load Py ultimate load Pu and ratio of Py/Pu are provided in Table V.

TABLE VI: Test results (Load Value Obtains Bytesting Machine)

Specimen	Yield load P_y (kN)	Ultimate load P_u (kN)	Ratio P_y/ P_u
PY-1D	400	524	0.76
PW-1D	440	520	0.85
PYGS-1D	400	546	0.73
PY-2D	660	777	0.85
PW-2D	720	840	0.86
PYGS-2D	660	720	0.92
PY-3D	800	1078	0.74
PW-3D	880	1189	0.74
PYGS-3D	800	987	0.81
ZY-1D	2828	3227	0.88
ZW-1D	2970	3190	0.93
ZY-2D	4553	4953	0.92
ZW-2D	4863	5260	0.92
ZY-3D	6187	8160	0.76
ZW-3D	6188	7779	0.80

B. Load-Displacement Response Results

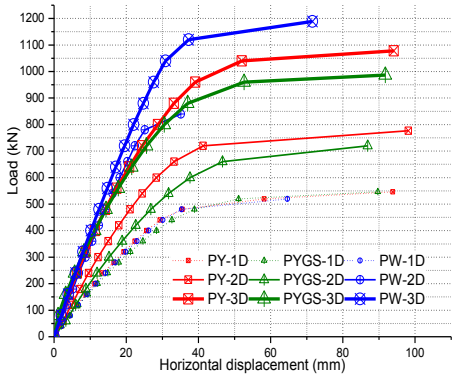

Fig. 8. Load displacement curve under eccentric compression test.

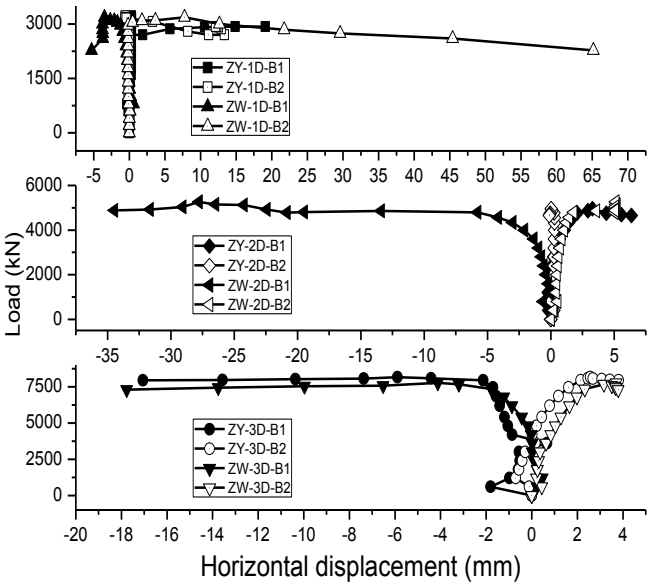

Fig. 9. Load displacement curve under axial compression test.
(B1 and B2 represent the two adjacent sides of the test column)

Fig. 8 shows the load displacement curve at the 1/2 height of the specimen. The specimen PW-3D had the maximum ultimate bearing capacity, 1189kN. The 10mm (-1D) thickness columns with the high-strength bolt joint, tapping joint and non-joint exhibited little difference in bearing capacity. Fig. 7 clearly indicates that as the column thickness increases, the bearing capacity of the non-nodal column (PW-2D and PW-3D) is the highest, the high-strength bolt joint column (PY-2D and PY-3D) is next, and the bolt tapping connection (PYGS-2D and PYGS-3D) is least. The bending stiffness of the non-nodal column was greater than that of the

joint column, which shows that the joint connection reduced the bearing capacity and stiffness of the column. But the curve's tendency indicates that the steel columns have better anti-deformation ability and strength.

Fig. 9 demonstrates the load displacement curve under the axial compression test. Specimen ZW-1D-B2 had the maximum displacement of 65mm. The initial horizontal slip curves of the columns with nodes are similar to those without nodes. With the increase of load, the initial horizontal slip of non-nodal columns clearly increases.

C. Load-Strain Response Results

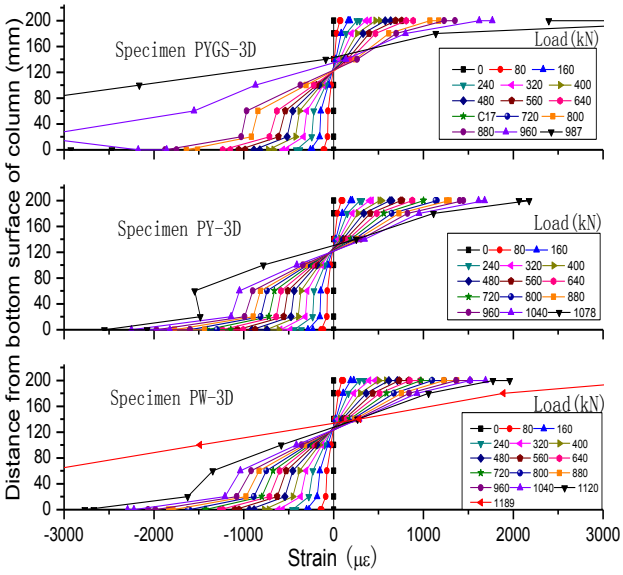

Fig. 10. Strain profiles of specimen PW-3D, PYGS-3D and PY-3D.

All specimens have a similar strain distribution along the height (distance from bottom surface of column) under eccentric compression. Here we take PW-3D, PYGS-3D and PY-3D as an example to investigate the strain profiles of specimens. As shown in Fig. 10, from load to failure, the strain of the specimens basically agreed with the plane section assumption. Also, the specimens were in a compression bending state. The failure form of the specimen was the yield of the column with no slip observed at the joint of the high-strength bolt, the tapping bolt or the flange plate. Accordingly, the shear force at the cross section of the column was small and the bolt was basically in a state of tension.

IV. Conclusion

This research team conducted an experimental investigation into the compressive behavior of fifteen steel columns. Based upon the test results obtained, the following significant conclusions were drawn:

1) The thickness of a steel column has significant influence on the compressive behavior of the composite beam. Specimens PW-3D, ZW-3D achieved the maximum ultimate bearing capacity, 1189kN, 8160kN, respectively.
2) Under the eccentric compression load, the bearing capacity of the high-strength bolt column and the bolt tapping rod column were slightly lower than those of the non-nodal column, but the eccentric compression load can be better transmitted. The failure mode of the columns was ductile failure.
3) Under the axial compression load, the bearing capacity of the high-strength bolt joint decreases slightly.
4) The failure mode of the columns under axial compression was steel column yield, but no failure of the high-strength bolt or the flange was observed. Therefore, such a modular assembly type of steel structure node can achieve the requirements of strong node and weak component.
5) Future experimental dynamic studies should be conducted to investigate the compressive behavior of steel columns with flange joints in the prefabricated steel frame structure.

Acknowledgment

Broad Homes Industrial Co. Ltd. financially supported this research. Furthermore, the authors wish to acknowledge the technical support of the National Engineering Laboratory for High Speed Railway Construction and the School of Civil Engineering, Central South University.

References

[1] R. Jiang, C. Wu, C. Mao, and C. Shrestha, ''Ecosystem visualization and analysis of Chinese prefabricated housing industry,'' *Procedia Engineering*, vol. 145, pp. 436-443, 2016.
[2] X. Liu, A. Xu, C. Sun, and C. Zhang, "Design study on a high-rise prefabricated steel frame structure with inclined braces," *Jianzhu Jiegou Xuebao (Journal of Building Structures)*, vol. 36, no. 5, pp. 54-62, May 2015.
[3] X. Liu, A. Zhang, J. Ma, Y. Tan, and Y. Bai, "Design and model test of a modularized prefabricated steel frame structure with inclined braces," *Advances in Materials Science and Engineering*, vol. 2015, pp. 1-12, October 2015.
[4] T. Zhou, Y. Guan, H. Wu, and L. Bai, "Research on vertical mechanical behavior of steel frame-prefabricated concrete lateral resistance wall fabricated structure," *Journal of Building Structures*, vol. 35, no. 9, pp. 27-34, September 2014.
[5] W. Zhao, G. Tong, and Q. Yang, "Experimental study on seismic behavior of steel frame with prefabricated reinforced concrete infill slit shear walls," *Journal of Building Structures*, vol. 33, no. 7, pp. 140-146, July 2012.
[6] Y. J. Yun, W. K. Hong, S. Kim, and J. T. Kim, "Experimental and analytical investigation of column-beam joints with smart frame based on strain compatibility," *International Journal of Engineering and Technology*, vol. 7, pp. 317-320, August 2015
[7] X. Liu, S. Pu, A. Zhang, A. Xu, Z. Ni, Y. Sun, and L. Ma, ''Static and seismic experiment for bolted-welded joint in modularized prefabricated steel structure,'' *Journal of Constructional Steel Research*, vol. 115, pp. 417-433, December 2015.
[8] L. Larusson, G. Fischer, and J. Jonsson, ''Prefabricated floor panels composed of fiber reinforced concrete and a steel substructure,'' *Engineering Structures*, vol. 46, pp. 104-115, January 2013.
[9] W. J. Zhao, Y. N. Guo, J. X. Tong, and S. M. Yuan, "Numerical simulation of prefabricated frame-shear wall structure with keyway connection of the column to wall under unidirectional horizontal load," *Applied Mechanics and Materials*, vol. 578-579, pp. 417-421, July 2014.
[10] *Metallic Materials - Tensile Testing at Ambient Temperature*, Chinese Standard GB/T 228-2002.

Jianjun Yang received his master and bachelor's degree from Beijing Jiaotong University. He is a distinguished professor at the School of Civil Engineering, Central South University. He focuses on various areas of research, such as steel structures, grid structures, prefabricated structures and structural health monitoring and evaluation.

Huaguo Chen received his bachelor's degree from Jiangxi University of Science and Technology. He is currently seeking his master's degree in structural engineering at the School of Civil Engineering, Central South University. He focuses on various areas of research, such as steel structures, grid structures, prefabricated structures and structural health monitoring and evaluation.

Jian Min received his master and bachelor's degree from Central South University. He is currently at China Construction Third Bureau First Engineering Co., Ltd. He focuses on structure design.